# Gaussian Beams For the Wave Equation

Nicolay M. Tanushev*

September 20, 2007

**Abstract**

High frequency solutions to partial differential equations (PDEs) are notoriously difficult to simulate numerically due to the large number of grid points required to resolve the wave oscillations. In applications, one often must rely on approximate solution methods to describe the wave field in this regime. Gaussian beams are asymptotically valid high frequency solutions concentrated on a single curve through the domain. We show that one can form integral superpositions of such Gaussian beams to generate more general high frequency solutions to PDEs.

As a particular example, we look at high frequency solutions to the constant coefficient wave equation. Since this PDE can be solved via a Fourier transform, we use the Fourier transform solution to gauge the error of Gaussian beam superposition solutions of several orders. Furthermore, we look at an example for which the solution exhibits a cusp caustic and investigate the order of magnitude of the wave amplitude as a function of frequency at the tip of the cusp. We show that the observed behavior is in agreement with the predictions of Maslov theory.

We also investigate the wave equation in the case of non-smooth sound speed and show how to construct an asymptotic solution using an incoming, reflected, and transmitted Gaussian beam. We use such solutions to derive Snell's law and determine the critical angle for total internal reflection. One can compute reflection and transmission coefficients from the asymptotic solution.

## 1 Introduction

Computation of high frequency waves is a necessity in many scientific applications. Fields requiring such computations include the semi-classical limit of the Schrödinger equation, communication networks, radio antenna engineering, laser optics, underwater acoustics, seismic wave propagation, and reflection seismology. These phenomena are modeled by partial differential equations (PDEs). The direct numerical integration of these PDEs is not computationally feasible, since one needs a tremendous number of grid points to resolve the rapid oscillations of the waves. As a result, one is forced to rely on approximate solutions which are valid in the high frequency regime.

Gaussian beams are approximate high frequency solutions to PDEs which are concentrated on a single ray through space-time. They derive their name from the fact that these solutions look like Gaussian distributions on planes perpendicular to the ray. The existence of such solutions has been known to the pure mathematics community since sometime in the 1960s and these solutions have been used to obtain results on propagation of singularities in PDEs ([6] and [7]). More general solutions that are not necessarily concentrated on a single ray can be obtained from a superposition of Gaussian beams. In the geophysical applications, Gaussian beam superpositions have been used to model the seismic wave field [1] and for seismic migration [5]. More recently, they have been used to model the stationary-in-time atmospheric waves that result from steady airflow over topography [8].

Gaussian beams are closely related to geometric optics, also known as the WKB method or ray-tracing. In both approaches, the solution of the PDE is assumed to be of the form,

$$e^{ik\phi}\left[a_0+\frac{1}{k}a_1+\ldots+\frac{1}{k^N}a_N\right] \ , \tag{1}$$

*Department of Mathematics, University of Texas at Austin, Austin, TX 78712. email: nicktan@math.utexas.edu

where $k$ is the high frequency parameter, $a_j$'s are the amplitude functions, and $\phi$ is the phase function. One then substitutes this form into the PDE to find the equations that the amplitudes and phase functions have to satisfy. Gaussian beams and geometric optics differ in the assumptions on the phase: the geometric optics method assumes that the phase is a real valued function, while the Gaussian beam construction does not.

Geometric optics has been widely used to model high frequency wave propagation in the applied mathematics community. A common problem with this method is that solving the equation for the phase using the method of characteristics leads to singularities which invalidate the approximation. Generally speaking, this breakdown occurs when nearby rays intersect resulting in a caustic where geometric optics incorrectly predicts that the amplitude of the solution is infinite.

The geometric optics solution can be extended past caustics, once they are identified, by Maslov's method. However, caustics can occur anywhere in the domain and their correction in numerical schemes is non-trivial. Intuitively speaking, Gaussian beams do not develop caustics since they are concentrated on a single ray, and one ray cannot develop a caustic. Thus, a Gaussian beam is a global solution of the PDE. Mathematically, this stems from the fact that the standard symplectic form and its complexification are preserved along the flow defined by the Hessian matrix of the phase. Hence, superpositions of Gaussian beams enjoy an advantage over geometric optics in that Gaussian beam solutions are global and their superposition provides a valid approximation at caustics wherever they occur.

Each Gaussian beam is constructed from a Taylor expansion of the phase and amplitude functions. The Taylor coefficients satisfy a system of ordinary differential equations (ODEs). In numerical simulations, once the numerical computations are complete, the wave field is given by a function. To obtain the highly oscillatory solution, this function is then evaluated at each grid point of the domain. Increasing the number of points in the domain simply means that this function needs to be evaluated at more points; no additional integration of the ODEs is required. In geometric optics approaches the wave field is calculated at points along rays in the domain. To increase the number of points in the domain, one has to either add more rays (which is usually numerically too expensive) or one has to interpolate the solution. This interpolation adds an additional layer of error to the geometric optics solution.

There are some tricks to limiting the interpolation error, such as inserting additional rays only where the rays paths are diverging. However, all of these improvements are accomplished through complicated numerical procedures. Geometric optics suffers from errors in the numerical ODE integration as well and from interpolating the solution. The interpolation errors are hard to quantify since they depend on properties of the function, such as its curvature, and on the location of the points used for interpolating.

The accuracy of the Gaussian beam solution is controlled by the continuous dependence on initial data estimates from well-posedness theory for the PDE. Usually, these estimates state that some norm of the error is bounded by a constant (which may depend on the time $t$) times some appropriate norm of the error in the initial data. Thus, the sources of error in the Gaussian beam solution are the error in approximating the initial data and the error in the numerical solution of the system of ODEs that define each beam. This gives the Gaussian beam solution a strong advantage over geometric optics, since it quantifies the error in the computed solution. Furthermore, since increasing the resolution of the solution can be accomplished without re-integration of the ODEs, one can easily examine a specific portion of the domain. In other words, the Gaussian beam solution provides an easy way to "zoom" into particular regions of the domain, which is a useful tool in applications.

In this paper we will consider Gaussian beam solutions to the constant coefficient wave equation,

$$\Box u \equiv u_{tt} - \triangle u = 0 \quad \text{in} \quad \mathbb{R}_+ \times \mathbb{R}^2 \ ,$$

with $u$ and $u_t$ given at $t = 0$.

This problem was chosen in particular, since it is easily solved using a Fourier transform. We will use this solution to benchmark the Gaussian beam solutions.

We will also consider the case of discontinuous sound speed for the wave equation,

$$u_{tt} - c(x)\triangle u \quad = \quad 0 \text{ in } \mathbb{R}_t \times \mathbb{R}^n_x \ ,$$

with $c$ smooth on either side of a codimension 1 hypersurface, but not smooth across it.

First, we begin by investigating superpositions of Gaussian beams.

## 2 Convergence of Gaussian Beam Superpositions

Throughout this section we will use the notation,

$$T_j^y[f](x)$$

to denote the $j^{th}$ order Taylor polynomial of $f$ about $y$ at the point $x$ and

$$R_j^y[f](x)$$

to denote its remainder. That is,

$$f(x) = T_j^y[f](x) + R_j^y[f](x) \ .$$

**Theorem 2.1.** *Let $\phi_0 \in C^\infty(\mathbb{R}^n)$ be a real-valued function, $a_0 \in C_0^\infty(\mathbb{R}^n)$, and $\rho \in C_0^\infty(\mathbb{R}^n)$ be such that $\rho \geq 0$, $\rho \equiv 1$ in a ball of radius $\delta > 0$ about the origin.*

*Define,*

$$\begin{aligned} u(x) &= a_0(x)e^{ik\phi_0(x)} \\ v(x;y) &= \left(\frac{k}{2\pi}\right)^{\frac{n}{2}} \rho(x-y)T_j^y[a_0](x)e^{ikT_{j+2}^y[\phi_0](x)-k|x-y|^2/2} \ . \end{aligned}$$

*Then*

$$\left\| \int_{\mathbb{R}^n} v(x;y)dy - u(x) \right\|_{L^2} \leq Ck^{-\frac{j+1}{2}} \ ,$$

*for some constant $C$.*

*Proof.* Estimating the norm, we have

$$\begin{aligned} \left\| \int_{\mathbb{R}^n} v(x;y)dy - u(x) \right\|_{L^2} &\leq \left\| \int_{\mathbb{R}^n} \left(\frac{k}{2\pi}\right)^{\frac{n}{2}} \rho(x-y)T_j^y[a_0](x)e^{ikT_{j+2}^y[\phi_0](x)-k|x-y|^2/2}dy - a_0(x)e^{ik\phi_0(x)} \right\|_{L^2} \\ &\leq \left\| \int_{\mathbb{R}^n} \left(\frac{k}{2\pi}\right)^{\frac{n}{2}} \rho(x-y)T_j^y[a_0](x)e^{-ikR_{j+2}^y[\phi_0](x)-k|x-y|^2/2}dy - a_0(x) \right\|_{L^2} \\ &\leq \left\| \left(\frac{k}{2\pi}\right)^{\frac{n}{2}} \int_{\mathbb{R}^n} \left[\rho(x-y)T_j^y[a_0](x) - a_0(x)\right] e^{-ikR_{j+2}^y[\phi_0](x)-k|x-y|^2/2}dy \right\|_{L^2} \\ &\qquad + \left\| \left(\frac{k}{2\pi}\right)^{\frac{n}{2}} \int_{\mathbb{R}^n} a_0(x) \left[e^{-ikR_{j+2}^y[\phi_0](x)} - 1\right] e^{-k|x-y|^2/2}dy \right\|_{L^2} \\ &:= I + J \ . \end{aligned}$$

We proceed by looking at the two pieces $I$ and $J$ independently. As

$$\begin{aligned} \rho(x-y)T_j^y[a_0](x) - a_0(x) &= (\rho(x-y)-1)a_0(x) + \rho(x-y)(T_j^y[a_0](x) - a_0(x)) \\ &= (\rho(x-y)-1)a_0(x) + \rho(x-y)R_j^y[a_0](x) \end{aligned}$$

we have:

$$\begin{aligned} I &\leq \left\| \left(\frac{k}{2\pi}\right)^{\frac{n}{2}} \int_{\mathbb{R}^n} |(\rho(x-y)-1)a_0(x)|\, e^{-k|x-y|^2/2}dy \right\|_{L^2} + \left\| \left(\frac{k}{2\pi}\right)^{\frac{n}{2}} \int_{\mathbb{R}^n} |\rho(x-y)R_j^y[a_0](x)| e^{-k|x-y|^2/2}dy \right\|_{L^2} \\ &\leq \left\| \left(\frac{k}{2\pi}\right)^{\frac{n}{2}} |a_0(x)| \int_{\mathbb{R}^n} \frac{|y|^{j+1}}{\delta^{j+1}} e^{-k|y|^2/2}dy \right\|_{L^2} + \left\| \left(\frac{k}{2\pi}\right)^{\frac{n}{2}} \int_{\mathbb{R}^n} \chi(x)C|y|^{j+1}e^{-k|y|^2/2}dy \right\|_{L^2} \\ &\leq Ck^{-\frac{j+1}{2}} \ , \end{aligned}$$

where $\chi(x) \in C_0^\infty(\mathbb{R}^n)$ such that $\chi(x) \geq 0$ and $\chi(x) \equiv 1$ for $x \in \{\mathrm{supp}(a_0) + \mathrm{supp}(\rho)\}$.

We now estimate $J$,

$$
\begin{aligned}
J &\le \left\| \left(\frac{k}{2\pi}\right)^{\frac{n}{2}} |a_0(x)| \int_{\mathbb{R}^n} \left[ \left|1-\cos(kR^y_{j+2}[\phi_0](x))\right|^2 \;+\; \left|\sin(kR^y_{j+2}[\phi_0](x))\right|^2 \right]^{1/2} e^{-k|x-y|^2/2} dy \right\|_{L^2} \\
&\le \left\| \left(\frac{k}{2\pi}\right)^{\frac{n}{2}} |a_0(x)| \int_{\mathbb{R}^n} 2k|R^y_{j+2}[\phi_0](x)| e^{-k|x-y|^2/2} dy \right\|_{L^2} \\
&\le \left\| \left(\frac{k}{2\pi}\right)^{\frac{n}{2}} |a_0(x)| \int_{\mathbb{R}^n} 2k|y|^{j+3} e^{-k|y|^2/2} dy \right\|_{L^2} \\
&\le Ck^{-\frac{j+1}{2}} \; .
\end{aligned}
$$

Thus,

$$
\left\| \int_{\mathbb{R}^n} v(x;y)dy - u(x) \right\|_{L^2} \quad \le \quad Ck^{-\frac{j+1}{2}} \; .
$$

$\square$

A result of this form also holds under much weaker assumptions on $\phi_0$ and $a_0$:

**Theorem 2.2.** *Let $\phi_0 \in C^2(\mathbb{R}^n)$ be a real-valued function and let $a_0 \in L^2(\mathbb{R}^n)$. For all $\epsilon > 0$, there exist functions $a$ and $\phi$ such that for sufficiently large $k$,*

$$
\left\| \int_{\mathbb{R}^n} v(x;y)dy - u(x) \right\|_{L^2} \quad \le \quad \epsilon \; ,
$$

*with*

$$
\begin{aligned}
u(x) &= a_0(x) e^{ik\phi_0(x)} \\
v(x;y) &= \left(\frac{k}{2\pi}\right)^{\frac{n}{2}} a(y) e^{ik\phi(x;y) - k|x-y|^2/2} \; .
\end{aligned}
$$

Before we proceed with the proof of this theorem, it is useful to record the following two lemmas.

**Lemma 2.3.** *For $f \in C_0^\infty$, let*

$$
f_k^*(x) = \left(\frac{k}{2\pi}\right)^{\frac{n}{2}} \int_{\mathbb{R}^n} f(y) e^{-ikR(x,y) - k|x-y|^2/2} dy \; ,
$$

*with $k > 0$ and $R$ a real valued function. Then*

$$
|f_k^*|_{L^2} \quad \le \quad |f|_{L^2}
$$

*Proof.* Note that

$$
\left(\frac{k}{2\pi}\right)^{\frac{n}{2}} \int_{\mathbb{R}^n} e^{-k|x-y|^2/2} dy \quad = \quad 1.
$$

Using the definition of $f_k^*$ and Hölder's inequality, we have:

$$
\begin{aligned}
|f_k^*(x)| &\le \int \left| \left(\frac{k}{2\pi}\right)^{\frac{n}{2}} e^{-ikR(x,y) - k|x-y|^2/2} f(y) \right| dy \\
&\le \int \left| \left(\frac{k}{2\pi}\right)^{\frac{n}{2}} e^{-k|x-y|^2/2} f(y) \right| dy \\
&\le \left[ \int |f(y)|^2 \left(\frac{k}{2\pi}\right)^{\frac{n}{2}} e^{-k|x-y|^2/2} dy \right]^{\frac{1}{2}} \left[ \int \left(\frac{k}{2\pi}\right)^{\frac{n}{2}} e^{-k|x-y|^2/2} dy \right]^{\frac{1}{2}} \\
&\le \left[ \int |f(y)|^2 \left(\frac{k}{2\pi}\right)^{\frac{n}{2}} e^{-k|x-y|^2/2} dy \right]^{\frac{1}{2}}
\end{aligned}
$$

Which implies that

$$|f_k^*(x)|^2 \quad \leq \quad \int |f(y)|^2 \left(\frac{k}{2\pi}\right)^{\frac{n}{2}} e^{-k|x-y|^2/2} dy$$

After integrating over $x$, we have

$$\|f_k^*\|_{L^2} \quad \leq \quad \|f\|_{L^2} \ .$$

□

**Lemma 2.4.** *Let $F \in C^2(\mathbb{R}^n;\mathbb{R})$. We have the following expansion for $F$:*

$$F(x) \quad = \quad F(y) + \nabla F(y)\cdot(x-y) + \frac{1}{2}(x-y)\cdot HF(y)(x-y) + R(x,y)\ ,$$

*where $HF(y)$ denotes the Hessian matrix of $F$ at $y$ and*

$$R(x,y) \quad = \quad (x-y)\cdot\left[\int_0^1 (1-t)[HF(tx+(1-t)y) - HF(y)]dt\right](x-y)\ .$$

*Proof.* Let $f \in C^2(\mathbb{R};\mathbb{R})$. By the Fundamental Theorem of Calculus and integration by parts, we have

$$\begin{aligned} f(t) - f(s) &= \int_s^t f'(\tau)d\tau \\ &= f'(s)(t-s) + \int_s^t f''(\tau)(t-\tau)d\tau\ . \end{aligned}$$

Thus,

$$\begin{aligned} f(t) &= f(s) + f'(s)(t-s) + \int_s^t f''(\tau)(t-\tau)d\tau \\ &= f(s) + f'(s)(t-s) + \frac{1}{2}f''(s)(t-s)^2 + r(t,s)\ , \end{aligned}$$

where

$$\begin{aligned} r(t,s) &= -\frac{1}{2}f''(s)(t-s)^2 + \int_s^t f''(\tau)(t-\tau)d\tau \\ &= \int_s^t \left[f''(\tau) - f''(s)\right](t-\tau)d\tau\ . \end{aligned}$$

Now for fixed $x$ and $y$, let

$$f(\sigma) = F(\sigma x + (1-\sigma)y)\ .$$

Applying the above expansion to this function for $s = 0$ and $t = 1$, we have

$$F(x) \quad = \quad F(y) + \nabla F(y)\cdot(x-y) + \frac{1}{2}(x-y)\cdot HF(y)(x-y) + R(x,y)\ ,$$

with

$$R(x,y) \quad = \quad (x-y)\cdot\left[\int_0^1 \left[HF(\tau x + (1-\tau)y) - HF(y)\right](1-\tau)d\tau\right](x-y)\ .$$

□

*Proof.* (Theorem 2.2) By Lemma 2.4 we have the following expansion for $\phi_0(x)$:

$$\phi_0(x) \quad = \quad \phi_0(y) + \nabla\phi_0(y)\cdot(x-y) + \frac{1}{2}(x-y)\cdot H\phi_0(y)(x-y) + R(x,y)\ ,$$

with $H\phi_0(y)$ and $R(x,y)$ as defined in the Lemma.

Now choose $a \in C_0^\infty(\mathbb{R}^n)$, such that $\|a_0 - a\|_{L^2} < \epsilon/2$, and define

$$\phi(x;y) \quad = \quad \phi_0(y) + \nabla\phi_0(y)\cdot(x-y) + \frac{1}{2}(x-y)\cdot H\phi_0(y)(x-y)\ ,$$

and

$$v(x;y) = \left(\frac{k}{2\pi}\right)^{\frac{n}{2}} a(y) e^{ik\phi(x;y)-k|x-y|^2/2}\ .$$

We now estimate,

$$\begin{aligned}
\left\|u(x) - \int_{\mathbb{R}^n} v(x;y)dy\right\|_{L^2} &= \left\|a_0(x)e^{ik\phi_0(x)} - \left(\frac{k}{2\pi}\right)^{\frac{n}{2}} \int_{R^n} a(y)e^{ik\phi(x;y)-k|x-y|^2/2}dy\right\|_{L^2} \\
&= \left\|e^{ik\phi_0(x)}\left[a_0(x) - \left(\frac{k}{2\pi}\right)^{\frac{n}{2}} \int_{\mathbb{R}^n} a(y)e^{-ikR(x,y)-k|x-y|^2/2}dy\right]\right\|_{L^2} \\
&\equiv \|a_0(x) - a_k^*(x)\|_{L^2} \\
&\leq \|a_0(x) - a(x)\|_{L^2} + \|a(x) - a_k^*(x)\|_{L^2} \\
&\leq \epsilon/2 + \|a(x) - a_k^*(x)\|_{L^2}\ .
\end{aligned}$$

Thus, we need to verify that $\|a - a_k^*\|_{L^2} \leq \epsilon/2$ as $k \to \infty$. First, we verify that it does so over a compact domain $\Omega$:

$$\begin{aligned}
\|a - a_k^*\|_{L^2,\Omega}^2 &= \int_\Omega \left|a(x) - \left(\frac{k}{2\pi}\right)^{\frac{n}{2}} \int_{\mathbb{R}^n} a(y)e^{-ikR(x,y)-k|x-y|^2/2}dy\right|^2 dx \\
&= \int_\Omega \left|\left(\frac{k}{2\pi}\right)^{\frac{n}{2}} \int_{R^n} \left[a(x) - a(y)e^{-ikR(x,y)}\right] e^{-k|x-y|^2/2}dy\right|^2 dx\ .
\end{aligned}$$

continuing the estimate, by Hölder's inequality, we have

$$\begin{aligned}
&\leq \left(\frac{k}{2\pi}\right)^{\frac{n}{2}} \int_\Omega \int_{R^n} \left|a(x) - a(y)e^{-ikR(x,y)}\right|^2 e^{-k|x-y|^2/2}dydx \\
&\leq 2\left(\frac{k}{2\pi}\right)^{\frac{n}{2}} \int_\Omega \int_{R^n} \left[|a(x)-a(y)|^2 + \left|a(y)\left(1 - e^{-ikR(x,y)}\right)\right|^2\right] e^{-k|x-y|^2/2}dydx\ .
\end{aligned}$$

and letting $(x-y) = z/k^{1/2}$ and eliminating $y$, we get

$$\begin{aligned}
&\leq 2\left(\frac{1}{2\pi}\right)^{\frac{n}{2}} \int_\Omega \int_{R^n} \left|a(x) - a(x - z/k^{1/2})\right|^2 e^{-|z|^2/2}dzdx \\
&\qquad + 2\left(\frac{1}{2\pi}\right)^{\frac{n}{2}} \int_\Omega \int_{R^n} \left|a(x - z/k^{1/2})\left(1 - e^{-ikR(x,x-z/k^{1/2})}\right)\right|^2 e^{-|z|^2/2}dzdx \\
&:= I + J
\end{aligned}$$

Let $D = \mathrm{supp}(a)$. Since $a$ is compactly supported and smooth,

- the measure of $D$ is finite, $\mu(D) < \infty$
- $|a(x)| < M$, for some $M > 0$
- $a$ is globally Lipschitz, $|a(x) - a(x - z/k^{1/2})| \leq L|z|/k^{1/2}$.

Estimating $I$ and $J$ independently, we have

$$\begin{aligned}
I &= 2\left(\frac{1}{2\pi}\right)^{\frac{n}{2}} \int_\Omega \int_{\mathbb{R}^n} \left|a(x) - a(x - z/k^{1/2})\right|^2 e^{-|z|^2/2}dzdx \\
&\leq 2\left(\frac{1}{2\pi}\right)^{\frac{n}{2}} \int_\Omega \int_{\mathbb{R}^n} \frac{L^2|z|^2}{k} e^{-|z|^2/2}dzdx \\
&\leq 2L^2\mu(\Omega)\left(\frac{1}{2\pi}\right)^{\frac{n}{2}} \int_{\mathbb{R}^n} \frac{|z|^2}{k} e^{-|z|^2/2}dz \\
&\leq \epsilon^2/32 \quad \text{for large enough} \quad k
\end{aligned}$$

We take a minute to estimate the remainder, $-ikR(x, x-\frac{z}{k^{1/2}})$, for large $k$. Let $r$ be large enough, so that

$$8M^2\mu(\Omega)\left(\frac{1}{2\pi}\right)^{\frac{n}{2}}\int_{|z|>r} e^{-|z|^2/2}dz \leq \epsilon^2/64$$

Then,

$$\begin{aligned}
&-ik\frac{z}{k^{1/2}}\cdot\left[\int_0^1(1-t)\left[H\phi_0(tx+(1-t)(x-\frac{z}{k^{1/2}}))-H\phi_0(x-\frac{z}{k^{1/2}})\right]dt\right]\frac{z}{k^{1/2}} \\
&\qquad\qquad = -iz\cdot\left[\int_0^1(1-t)\left[H\phi_0(x+(t-1)\frac{z}{k^{1/2}})-H\phi_0(x-\frac{z}{k^{1/2}})\right]dt\right]z\ .
\end{aligned}$$

Since $H\phi_0$ is continuous, it is uniformly continuous over compact sets in $(x, z)$. Thus, for $|z| \leq r$ and every $\delta > 0$, for sufficiently large $k$, we have,

$$|-ikR(x, x-z/k^{1/2})| \quad < \quad \delta\ .$$

Thus for small enough $\delta$, we have the following estimate for $J$:

$$\begin{aligned}
J \quad &\leq \quad 2\left(\frac{1}{2\pi}\right)^{\frac{n}{2}}\int_\Omega\int_{|z|\leq r}\left|a(x-z/k^{1/2})(1-e^{-ikR(x,x-z/k^{1/2})})\right|^2 e^{-|z|^2/2}dzdx \\
&\qquad + \quad 8M^2\left(\frac{1}{2\pi}\right)^{\frac{n}{2}}\int_\Omega\int_{|z|>r} e^{-|z|^2/2}dzdx \\
&\leq \quad 2\left(\frac{1}{2\pi}\right)^{\frac{n}{2}} M^2\mu(\Omega)\mu(\{z:|z|\leq r\})(|1-\cos(\delta)|^2+|\sin(\delta)|^2)+\epsilon^2/64 \\
&\leq \quad \epsilon^2/32
\end{aligned}$$

Putting all of these estimates together, we see that

$$\begin{aligned}
\|a-a_k^*\|^2_{L^2,\Omega} \quad &\leq \quad \epsilon^2/32+\epsilon^2/32 \\
&\leq \quad \epsilon^2/16
\end{aligned}$$

and

$$\begin{aligned}
\|a-a_k^*\|_{L^2} \quad &= \quad \|a-a_k^*\|_{L^2,D}+\|a-a_k^*\|_{L^2,D^c} \\
&\leq \quad \epsilon/4+\|a_k^*\|_{L^2,D^c} \\
&\leq \quad \epsilon/4+\|a_k^*\|_{L^2}-\|a_k^*\|_{L^2,D} \\
&\leq \quad \epsilon/4+\|a\|_{L^2}-\|a_k^*\|_{L^2,D} \\
&\leq \quad \epsilon/4+\|a\|_{L^2,D}-\|a_k^*\|_{L^2,D} \\
&\leq \quad \epsilon/4+\|a-a_k^*\|_{L^2,D} \\
&\leq \quad \epsilon/4+\epsilon/4 \\
&\leq \quad \epsilon/2\ ,
\end{aligned}$$

where we have used Lemma 2.3. Thus, for large enough $k$,

$$\begin{aligned}
\|u(x)-\int_{\mathbb{R}^n} v(x;y)dy\|_2 \quad &\leq \quad \epsilon/2+\|a(x)-a_k^*(x)\|_{L^2} \\
&\leq \quad \epsilon\ ,
\end{aligned}$$

which proves the result.

$\square$

## 3 Constant Coefficient Wave Equation

In this section, we investigate Gaussian beam solutions to the constant coefficient wave equation,

$$\Box u \equiv u_{tt} - \triangle u = 0 \quad \text{in} \quad \mathbb{R}_+ \times \mathbb{R}^2 \ , \tag{2}$$

with $u$ and $u_t$ given at $t = 0$. This problem was chosen in particular, since it is easily solved using a Fourier transform. The solution of the initial value problem can be immediately written in terms of the Fourier transform in the space variables $x$ of the initial data ($\eta$ is the dual variable):

$$u_F = \frac{1}{2}\mathcal{F}^{-1}\left\{\mathcal{F}\{u_0\}\left(e^{i|\eta|t} + e^{-i|\eta|t}\right) + \frac{\mathcal{F}\{u_{0t}\}}{i|\eta|}\left(e^{i|\eta|t} - e^{-i|\eta|t}\right)\right\} \ .$$

We will use the Fourier Transform solution to benchmark the Gaussian beam solutions.

The wave equation (2) is well-posed and we have the following estimate for the solution.

**Theorem 3.1.** *Let $u$ satisfy*

$$\begin{aligned} u_{tt} - \triangle u = F(t,x) \quad & \textit{in} \quad [0,T] \times \mathbb{R}^n \\ u = f(x) \quad & \textit{for} \quad t = 0 \\ u_t = g(x) \quad & \textit{for} \quad t = 0 \ , \end{aligned}$$

*with $F$, $f$ and $g$ compactly supported. Then,*

$$\|u\|^2_{L^2(\mathbb{R}^n)} + \|u_t\|^2_{L^2(\mathbb{R}^n)} \leq \frac{e^T}{2}\left[\|f\|^2_{H^1(\mathbb{R}^n)} + \|g\|^2_{L^2(\mathbb{R}^n)} + \|F\|^2_{L^2([0,T]\times\mathbb{R}^n)}\right] \ ,$$

*for $t \in [0,T]$.*

*Proof.* Let $\Omega \subset \mathbb{R}^n$ be a bounded domain with a smooth boundary, such that $u(t,x) \equiv 0$ for $(t,x) \in [0,T] \times \overline{\Omega^c}$. The existence of such a domain is guaranteed by finite speed of propagation for the wave equation and the fact that $F$, $f$ and $g$ are all compactly supported. Define

$$E(t) = \frac{1}{2}\int_\Omega \left(|u_t|^2 + |\nabla u|^2\right) dx \ .$$

Now,

$$\begin{aligned} \frac{d}{dt}E(t) &= \int_\Omega (u_t u_{tt} + \nabla u \cdot \nabla u_t) \ dx \\ &= \int_\Omega (u_t u_{tt} - u_t \triangle u) \ dx \\ &= \int_\Omega u_t F \ dx \\ &\leq \frac{1}{2}\int_\Omega |u_t|^2 \ dx + \frac{1}{2}\int_\Omega |F|^2 \ dx \\ &\leq E(t) + \frac{1}{2}\int_\Omega |F|^2 \ dx \end{aligned}$$

By Gronwall's inequality (see [3] appendix B),

$$\begin{aligned} E(t) &\leq e^{\int_0^t 1 ds}\left[E(0) + \frac{1}{2}\int_0^t \int_\Omega |f(s,x)|^2 \ dx \ ds\right] \\ &\leq \frac{e^T}{2}\left[\|f\|^2_{H^1(\mathbb{R}^n)} + \|g\|^2_{L^2(\mathbb{R}^n)} + \|F\|^2_{L^2([0,T]\times\mathbb{R}^n)}\right] \ . \end{aligned}$$

□

## 3.1 Gaussian Beam Solutions

**Phase and Amplitude Equations** Upon substituting the ansatz,

$$u = e^{ik\phi}\left[a + \frac{1}{k}b\right] , \tag{3}$$

into

$$u_{tt} - \triangle u = 0 \tag{4}$$

and collecting powers of the large parameter, $k$, we obtain the following equations for the phase and amplitudes:

$$\begin{aligned}
k^2 &: \quad (-\phi_t^2 + \phi_{x_1}^2 + \phi_{x_2}^2)a = 0 \\
k^1 &: \quad 2i(\phi_t a_t - \phi_{x_1} a_{x_1} - \phi_{x_2} a_{x_2}) + i(\phi_{tt} - \phi_{x_1 x_1} - \phi_{x_2 x_2})a + (-\phi_t^2 + \phi_{x_1}^2 + \phi_{x_2}^2)b = 0 \\
k^0 &: \quad 2i(\phi_t b_t - \phi_{x_1} b_{x_1} - \phi_{x_2} b_{x_2}) + i(\phi_{tt} - \phi_{x_1 x_1} - \phi_{x_2 x_2})b + (a_{tt} - a_{x_1 x_1} - a_{x_2 x_2}) = 0 .
\end{aligned}$$

These equations simplify to:

$$\begin{aligned}
2(\phi_t \phi_t - \phi_{x_1}\phi_{x_1} - \phi_{x_2}\phi_{x_2}) &= 0 \\
2(\phi_t a_t - \phi_{x_1} a_{x_1} - \phi_{x_2} a_{x_2}) &= -a\Box\phi \\
2(\phi_t b_t - \phi_{x_1} b_{x_1} - \phi_{x_2} b_{x_2}) &= i\Box a - b\Box\phi .
\end{aligned} \tag{5}$$

The first equation is called the eikonal equation and the others are referred to as the transport equations. Since these equations hold everywhere, we use them (and their derivatives) to determine the initial data for $u_t$ at $t = 0$. In other words, we take

$$\Phi_t = \pm\sqrt{|\nabla_x \Phi|} , \tag{6}$$

where $\nabla_x = (\partial_{x_1}, \partial_{x_2})$. Also,

$$A_t = \frac{2\nabla_x\Phi \cdot \nabla_x A - A\Box\Phi}{2\Phi_t} , \tag{7}$$

and so on.

In the spirit of the Gaussian beam construction (see Appendix A.1 of [8], or section 2.1 of [7]), we will not look for approximate global solutions of these equations. We will solve them on a single characteristic originating from a point $y = (y_1, y_2)$ on the initial data surface $t = 0$. Recall that the Gaussian beam construction relies on equations (5) to hold to high order on the characteristic. That is, they hold along with several of their derivatives. We use these equations to define the phase and amplitudes along with several of their derivatives on the characteristic and then we define these functions globally through a Taylor expansion and a localizing cut-off function.

The accuracy of the Gaussian beam superposition solution depends on the accuracy of the individual beams. Two factors that control this accuracy are

- the number of terms in the Taylor expansions for the phase and amplitudes,
- the number of terms in the ansatz (1).

These two factors are not independent. As can be seen in the construction of Gaussian beams, the Taylor coefficients of each one of the amplitudes in the ansatz (1) depends on the coefficients of the previous amplitudes and the phase. In other words, we can't define arbitrarily many Taylor coefficients for the $a_j$ amplitude without a certain number of the coefficients of the $a_l$ amplitudes for $l = 0 \ldots (j-1)$ and of the phase $\phi$. On the other hand, while we can define the Taylor coefficients of the phase without any of the amplitude coefficients, taking many coefficients is unnecessary, since eventually their overall effect on the accuracy of the Gaussian beam solution is smaller than that of amplitudes that have been omitted by truncating the asymptotic expansion of the ansatz (1) at $N$. We keep these two competing factors in mind when defining the higher order Gaussian beams in the next several sections.

**First Order Gaussian Beam Solution** To obtain a Gaussian Beam solution, as a bare minimum, we must take terms up to $2^{\text{nd}}$ order for $\phi$ and up to $0^{\text{th}}$ order for the first amplitude function $a$ in their respective Taylor expansions. We refer to this as a "first" order Gaussian beam. The equations for the characteristic $(\mathcal{T}, \mathcal{X})$ originating from $y$ at $t = 0$ are

$$\begin{array}{rclcrcl} \dot{\mathcal{T}} & = & 2\tau & \qquad & \mathcal{T}(0) & = & 0 \\ \dot{\mathcal{X}} & = & -2\xi & & \mathcal{X}(0) & = & y = (y_1, y_2) \\ \dot{\tau} & = & 0 & & \tau(0) & = & \Phi_t(y) \\ \dot{\xi} & = & 0 & & \xi(0) & = & \nabla_y \Phi(y) \end{array} \tag{8}$$

where $\dot{}$ signifies differentiation with respect to the ray parameter $s$. Also, recall that $\tau = \phi_t$ and $\xi = \nabla_x \phi$.

Proceeding, we get an equation for $\phi$,

$$\dot{\phi} \;=\; 0 \qquad \phi(0) \;=\; \Phi(y) \;, \tag{9}$$

and its second derivatives,

$$\dot{\phi}_{\alpha\beta} \;=\; -2\phi_{t\alpha}\phi_{t\beta} + 2\phi_{x_1\alpha}\phi_{x_1\beta} + 2\phi_{x_2\alpha}\phi_{x_2\beta} \;,$$

where $\alpha$ and $\beta$ stand for any one of $t$, $x_1$ or $x_2$. The initial conditions are,

$$(\phi_{\alpha\beta}) \;=\; \begin{pmatrix} * & * & * \\ * & \Phi_{x_1x_1} + i & \Phi_{x_1x_2} \\ * & \Phi_{x_1x_2} & \Phi_{x_2x_2} + i \end{pmatrix} \;,$$

where the $*$'s are chosen so that

$$\begin{gathered} \phi_{\alpha\beta} = \phi_{\beta\alpha} \\ 0 = \dot{\phi}_{\alpha} = 2\phi_t\phi_{t\alpha} - 2\phi_{x_1}\phi_{x_1\alpha} - 2\phi_{x_2}\phi_{x_2\alpha} \;. \end{gathered}$$

Note that the equations for the second derivatives of $\phi$ are non-linear. One can rewrite them as a non-linear Ricatti matrix equation. Even though this matrix equation is also non-linear, for the initial condition that we have chosen, there exists a global solution. One shows this by rewriting the Ricatti equations in terms of two of linear matrix equations (see Appendix A.1 of [8], or section 2.1 of [7]). Although, one can use these two linear equations to compute the second derivatives of $\phi$, it is more advantageous in simulations to integrate the non-linear version of the equations, since there are fewer equations and there is no need to invert a matrix.

Finally, we have the transport equation,

$$\dot{a} \;=\; -a\Box\phi \qquad a(0) \;=\; A(y) \;.$$

**Second Order Gaussian Beam Solution** A "second" order Gaussian beam has terms up to $3^{\text{rd}}$ order for the phase and up to $1^{\text{st}}$ order for the first amplitude $a$. As before, we obtain equations for these quantities by differentiating the eikonal and transport equations (again, $\alpha$, $\beta$ and $\gamma$ can be any one of $t$, $x_1$ or $x_2$),

$$\dot{\phi}_{\alpha\beta\gamma} \;=\; -2\phi_{t\gamma}\phi_{t\alpha\beta} + 2\phi_{x_1\gamma}\phi_{x_1\alpha\beta} + 2\phi_{x_2\gamma}\phi_{x_2\alpha\beta} + \partial_\gamma\left(-2\phi_{t\alpha}\phi_{t\beta} + 2\phi_{x_1\alpha}\phi_{x_1\beta} + 2\phi_{x_2\alpha}\phi_{x_2\beta}\right) \;.$$

The initial conditions for these equations come from evaluating the equations in the previous section at $\mathcal{T} = 0$.

The equations for the derivatives of the first amplitude are,

$$\dot{a}_\alpha \;=\; -2a_t\phi_{t\alpha} + 2a_{x_1}\phi_{x_1\alpha} + 2a_{x_2}\phi_{x_2\alpha} + \partial_\alpha(-a\Box\phi) \;.$$

Again, initial conditions are obtained by evaluating the equations from the previous sections at $\mathcal{T} = 0$.

**Third Order Gaussian Beam Solution** A "third" order Gaussian beam has terms up to $4^{\text{th}}$ order for the phase, up to $2^{\text{nd}}$ order for the first amplitude $a$, and up to $0^{\text{th}}$ order for the second amplitude $b$. The equations are as follows ($\alpha$, $\beta$, $\gamma$ and $\delta$ can be any one of $t$, $x_1$ or $x_2$):

$$\begin{aligned} \dot{\phi}_{\alpha\beta\gamma\delta} \;=\; & -2\phi_{t\delta}\phi_{t\alpha\beta\gamma} + 2\phi_{x_1\delta}\phi_{x_1\alpha\beta\gamma} + 2\phi_{x_2\delta}\phi_{x_2\alpha\beta\gamma} \\ & +\partial_\delta\left(-2\phi_{t\gamma}\phi_{t\alpha\beta} + 2\phi_{x_1\gamma}\phi_{x_1\alpha\beta} + 2\phi_{x_2\gamma}\phi_{x_2\alpha\beta}\right) \\ & +\partial_{\delta\gamma}\left(-2\phi_{t\alpha}\phi_{t\beta} + 2\phi_{x_1\alpha}\phi_{x_1\beta} + 2\phi_{x_2\alpha}\phi_{x_2\beta}\right) \;, \end{aligned}$$

$$
\begin{aligned}
\dot{a}_{\alpha\beta} &= -2a_{t\alpha}\phi_{t\beta} + 2a_{x_1\alpha}\phi_{x_1\beta} + 2a_{x_2\alpha}\phi_{x_2\beta} \\
&\quad + \partial_\beta\left(-2a_t\phi_{t\alpha} + 2a_{x_1}\phi_{x_1\alpha} + 2a_{x_2}\phi_{x_2\alpha}\right) \\
&\quad + \partial_{\alpha\beta}(-a\Box\phi) \ ,
\end{aligned}
$$

$$
\dot{b} = i\Box a - b\Box\phi \ .
$$

The initial conditions are $b(0,y) = B(y)$ and the rest come from evaluating the equations of the previous section at $\mathcal{T} = 0$.

**Superpositions** After the equations for the various phase and amplitude Taylor coefficients have been solved, we know the characteristic path, $(\mathcal{T}(s;y), \mathcal{X}(s;y))$, which originates from $(0, y_1, y_2)$. Evaluating all of the Taylor coefficients and paths for $s$ so that $T(s;y) = t$, we can define the following Gaussian beams:

$$
\begin{aligned}
v_1(t,x;y) &= \rho(x-\mathcal{X})\left[T_0^{\mathcal{X}}[a](x)\right] e^{ikT_2^{\mathcal{X}}[\phi](x)} \\
v_2(t,x;y) &= \rho(x-\mathcal{X})\left[T_1^{\mathcal{X}}[a](x)\right] e^{ikT_3^{\mathcal{X}}[\phi](x)} \\
v_3(t,x;y) &= \rho(x-\mathcal{X})\left[T_2^{\mathcal{X}}[a](x) + \frac{1}{k}T_0^{\mathcal{X}}[b](x)\right] e^{ikT_4^{\mathcal{X}}[\phi](x)},
\end{aligned}
$$

where $T_n^Y[f](z)$ is the $n$-th order Taylor polynomial of $f$ about $Y$ evaluated at $z$ and $\rho$ is a cut-off function such that on its support the Taylor expansion of $\phi$ has a positive imaginary part. We form the superpositions,

$$
u_j(t,x) = \frac{k}{2\pi}\int_{\text{supp}\{a_0\}} v_j(t,x;y)dy \ , \tag{10}
$$

for $j = 1, 2, 3$. As the $v_j$'s are asymptotic solutions of the wave equation, so will be their superpositions $u_j$. All that remains to check is that these superpositions accurately approximate the initial data. Evaluating at $t = 0$ we find that,

$$
\begin{aligned}
v_1(0,x;y) &= \rho(x-y)e^{ikT_2^y[\Phi](x) - k|x-y|^2/2}\left(T_0^y[A](x)\right) \\
v_2(0,x;y) &= \rho(x-y)e^{ikT_3^y[\Phi](x) - k|x-y|^2/2}\left(T_1^y[A](x)\right) \\
v_3(0,x;y) &= \rho(x-y)e^{ikT_4^y[\Phi](x) - k|x-y|^2/2}\left(T_2^y[A](x) + \frac{1}{k}T_0^y[B](x)\right) \ .
\end{aligned}
$$

Note that differentiating these expressions in $x$ will either bring a factor of $k$ or lower the order of the Taylor expansion for the amplitude by 1. Differentiating $\rho$ yields an expression which vanishes in a neighborhood of $y$, so this term is smaller than any inverse power of $k$ in the superposition as $k \to \infty$. Thus, by applying Theorem 2.1, we have

$$
\begin{aligned}
\|u_1|_{t=0} - u_0\|_{H^1} &\leq Ck^{-1/2+1} \\
\|u_2|_{t=0} - u_0\|_{H^1} &\leq Ck^{-1+1} \\
\|u_3|_{t=0} - u_0\|_{H^1} &\leq Ck^{-3/2+1} \ .
\end{aligned}
$$

We also need to look at the initial data for the time derivative of the solution. We compute,

$$
\begin{aligned}
\partial_t v_1(t,x;y) &= \frac{ds}{dt}\Big[ik\rho(x-\mathcal{X})T_0^{\mathcal{X}}[a](x)\left(T_2^{\mathcal{X}}[\dot{\phi}](x) - \dot{\mathcal{X}}_j T_1^{\mathcal{X}}[\phi_{x_j}](x)\right) \\
&\qquad - \dot{\mathcal{X}}_j\rho_{x_j}(x-\mathcal{X})T_0^{\mathcal{X}}[a](x) + \rho(x-\mathcal{X})T_0^{\mathcal{X}}[\dot{a}](x)\Big] e^{ikT_2^{\mathcal{X}}[\phi](x)} \ .
\end{aligned}
$$

Recognizing that,

$$
\frac{ds}{dt}\left(T_j^{\mathcal{X}}[\dot{f}](x) - \dot{\mathcal{X}}_l T_{j-1}^{\mathcal{X}}[f_{x_l}](x)\right) = T_{j-1}^{\mathcal{X}}[f_t](x) + E_j \ ,
$$

where $E_j$ is a remainder term that is $O(|x-\mathcal{X}|^j)$ and evaluating at $t = 0$, we have

$$
\partial_t v_1(0,x;y) = \left[ik\rho(x-y)T_0^y[A](x)T_1^y[\Phi_t](x) + O(k|x-y|^2+1)\ \right] e^{ikT_2^y[\Phi](x) - k|x-y|^2/2} \ .
$$

Similarly, we compute,

$$\begin{aligned}\partial_t v_2(t,x;y) &= \frac{ds}{dt}\Big[ik\rho(x-\mathcal{X})T_1^{\mathcal{X}}[a](x)\left(T_3^{\mathcal{X}}[\dot\phi](x)-\dot{\mathcal{X}}_j T_2^{\mathcal{X}}[\phi_{x_j}](x)\right)\\ &\quad +\rho(x-\mathcal{X})\left(T_1^{\mathcal{X}}[\dot a](x)-\dot{\mathcal{X}}_j T_0^{\mathcal{X}}[a_{x_j}](x)\right)\\ &\quad -\dot{\mathcal{X}}_j\rho_{x_j}(x-\mathcal{X})T_1^{\mathcal{X}}[a](x)\Big]\, e^{ikT_3^{\mathcal{X}}[\phi](x)}\ ,\end{aligned}$$

and

$$\begin{aligned}\partial_t v_3(t,x;y) &= \frac{ds}{dt}\Big[\quad ik\rho(x-\mathcal{X})\left(T_2^{\mathcal{X}}[a](x)+\frac{1}{k}T_0^{\mathcal{X}}[b](x)\right)\left(T_4^{\mathcal{X}}[\dot\phi](x)-\dot{\mathcal{X}}_j T_3^{\mathcal{X}}[\phi_{x_j}](x)\right)\\ &\quad +\rho(x-\mathcal{X})\left(T_2^{\mathcal{X}}[\dot a](x)-\dot{\mathcal{X}}_j T_1^{\mathcal{X}}[a_{x_j}](x)\right)+\frac{1}{k}\rho(x-\mathcal{X})T_0^{\mathcal{X}}[\dot b](x)\\ &\quad -\dot{\mathcal{X}}_j\rho_{x_j}(x-\mathcal{X})\left(T_2^{\mathcal{X}}[a](x)+\frac{1}{k}T_0^{\mathcal{X}}[b](x)\right)\Big]\, e^{ikT_4^{\mathcal{X}}[\phi](x)}\ .\end{aligned}$$

Again, substituting and evaluating at $t=0$, we have

$$\begin{aligned}\partial_t v_2(0,x;y) &= \big[ik\rho(x-y)T_1^y[A](x)T_2^y[\Phi_t](x)+O(k|x-y|^3)\\ &\quad +\rho(x-y)T_0^y[A_t](x)+O(|x-y|)\\ &\quad +O(|x-y|^\infty)\big]\, e^{ikT_3^y[\Phi](x)-k|x-y|^2/2}\ ,\end{aligned}$$

and

$$\begin{aligned}\partial_t v_3(0,x;y) &= \Big[ik\rho(x-y)\left(T_2^y[A](x)+\frac{1}{k}T_0^y[B](x)\right)\left(T_3^y[\Phi_t](x)+O(|x-y|^4)\right)\\ &\quad +\rho(x-y)T_1^y[A_t](x)+O(|x-y|^2+k^{-1})\\ &\quad +O(|x-y|^\infty)\Big]\, e^{ikT_4^y[\Phi](x)-k|x-y|^2/2}\ .\end{aligned}$$

Thus, by applying Theorem 2.1 and using the ideas of its proof, we have

$$\begin{aligned}\|\partial_t u_1|_{t=0}-u_{0t}\|_{H^1} &\le Ck^{1/2+1}\\ \|\partial_t u_2|_{t=0}-u_{0t}\|_{H^1} &\le Ck^{1}\\ \|\partial_t u_3|_{t=0}-u_{0t}\|_{H^1} &\le Ck^{-1/2+1}\ .\end{aligned}$$

## 3.2 Simple Example of an Initial Value Problem: Traveling Waves

We choose the initial data for the PDE (2) to be,

$$u_0=u|_{t=0}=e^{ik\Phi(x)}\left[A(x)+\frac{1}{k}B(x)\right]\ ,$$

where

$$\begin{aligned}\Phi(x) &= x^5+y^5+x^3+y^3+x+y\\ A(x) &= \sin(x)\\ B(x) &= 0\ ,\end{aligned}$$

and,

$$u_{0t}=u_t|_{t=0} = e^{ik\Phi}\left[ik\Phi_t\left(A+\frac{1}{k}B\right)+A_t+\frac{1}{k}B_t\right]\ ,$$

where $\Phi_t$, $A_t$ and $B_t$ are determined by the equations in section 3.1 to give waves that propagate in only one direction (i.e. with positive square root in equation (6)). We also fix the high frequency parameter $k=200$.

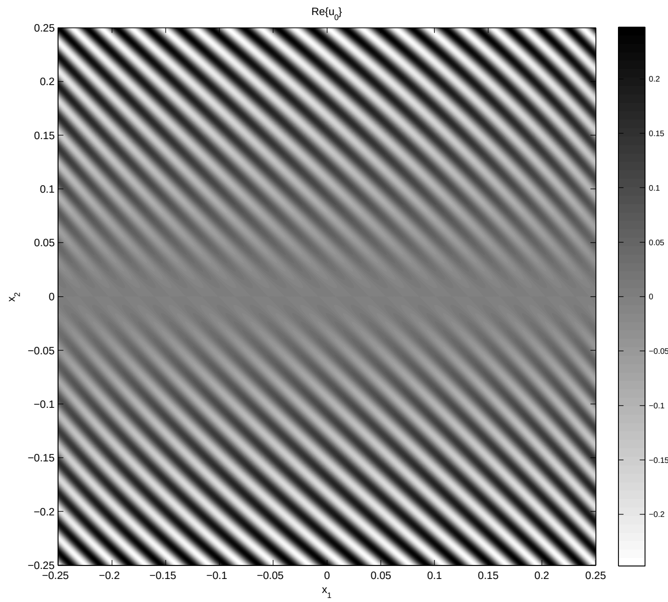


**Figure 1:** Initial data for the wave equation: Traveling Waves

**Comparisons** The numerical calculations of the Fourier transform solution and the Gaussian beam superpositions were carried out using a combination of Matlab and C. The Fourier transform solution will be used as the "true" solution to find the error in the wave field that is present in the Gaussian beam superpositions. Figure 2 shows the absolute value of the difference between the Fourier transform solution and the Gaussian beam superpositions along $x_2 = 0$ at $t = 0$, while Figure 3 shows the same difference at $t = 0.2$. The numerically computed norms of the differences are given in Table 1. As suggested by theorem 2.1, the approximation of the initial data improves significantly with the addition of more terms in the Taylor expansions.

| | Difference at $t = 0$ | | Difference at $t = 0.2$ | |
|---|---|---|---|---|
| | $L_2$-norm | $H_1$-norm | $L_2$-norm | $H_1$-norm |
| $1^{\text{st}}$ order | 0.011244 | 3.3744 | 0.017219 | 5.9586 |
| $2^{\text{nd}}$ order | 0.0012426 | 0.37761 | 0.0051799 | 1.8206 |
| $3^{\text{rd}}$ order | $7.7548 \times 10^{-6}$ | 0.0023186 | 0.0019411 | 0.68523 |

**Table 1:** Norm differences between the Fourier transform solution and the Gaussian beam superpositions for the traveling waves example.

## 3.3 Initial Value Problem for an Expanding Ring of Waves

We choose the initial data for the PDE (2) to be,

$$u_0 = u|_{t=0} = e^{ik\Phi(x)} \left[ A(x) + \frac{1}{k} B(x) \right] ,$$

where

$$\begin{aligned} \Phi(x) &= \frac{1}{2}\left(1 - \sqrt{x_1^2 + x_2^2}\right) \\ A(x) &= \begin{cases} \exp\left((10(|x|-1)^2 - 1)^{-1} + 1\right) & \text{for } 10(|x|-1)^2 < 1 \\ 0 & \text{otherwise} \end{cases} \\ B(x) &= 0 \, , \end{aligned}$$

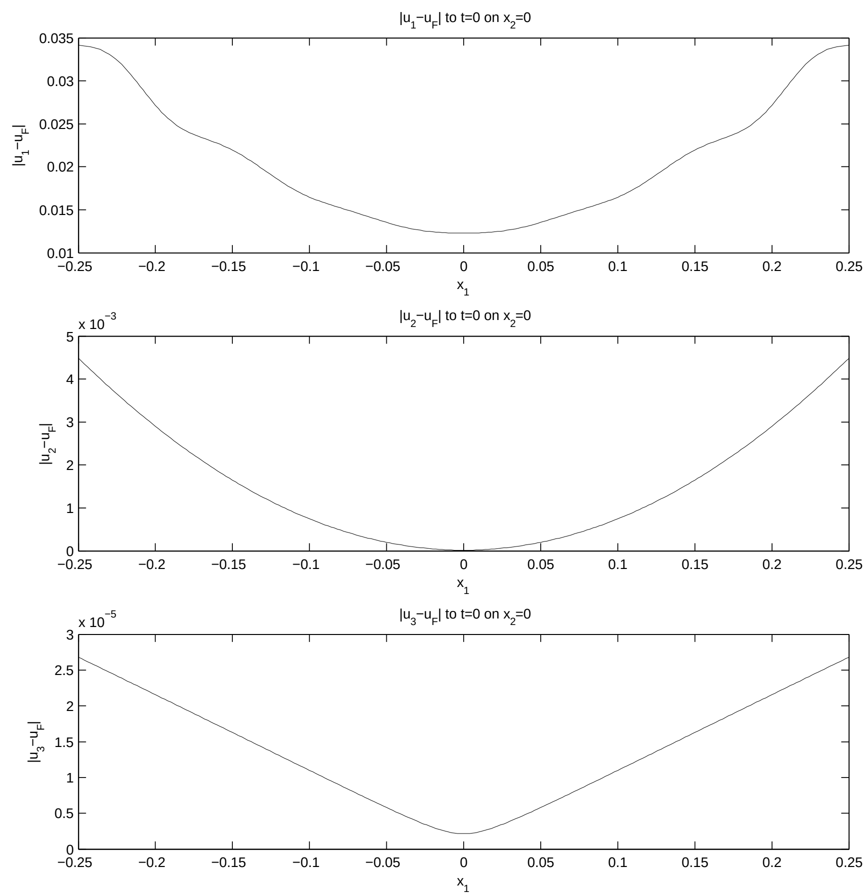


**Figure 2:** Differences between the Fourier transform solution and the Gaussian beam superposition solutions at $t = 0$ for $x_2 = 0$ for the traveling waves example. Note that the scale for each graph is different.

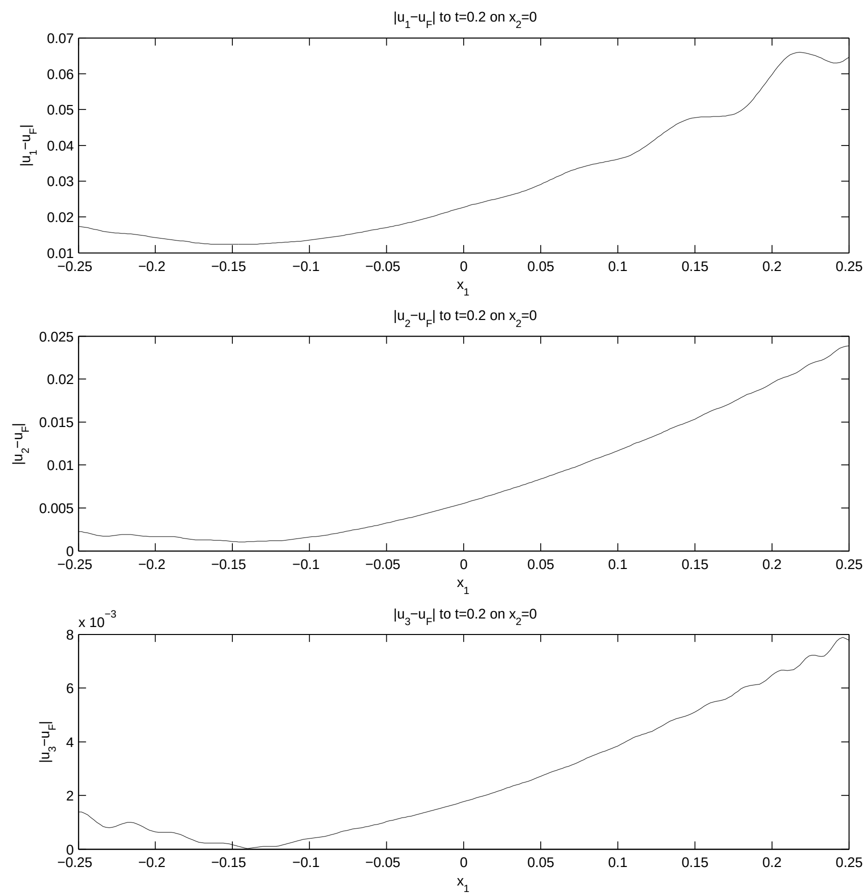


**Figure 3:** Differences between the Fourier transform solution and the Gaussian beam superposition solutions at $t = 0.2$ for $x_2 = 0$ for the traveling waves example.

and,

$$u_{0t} = u_t|_{t=0} \quad = \quad e^{ik\Phi}\left[ik\Phi_t\left(A + \frac{1}{k}B\right) + A_t + \frac{1}{k}B_t\right] ,$$

where $\Phi_t$, $A_t$ and $B_t$ are determined by the equations in section 3.1 to give an expanding ring of waves. This amounts to taking the positive square root in equation (6). We also fix the high frequency parameter $k = 500$.

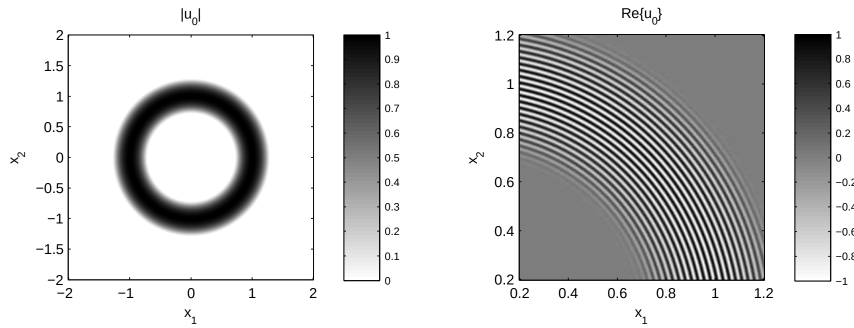


**Figure 4:** Initial data for the wave equation: ring of expanding waves.

Figure 5 shows a set of characteristics with $|y| = 1$ for $\mathcal{T} = 0$ to 6 for the expanding ring of waves example. Note that the characteristics are spreading apart quickly.

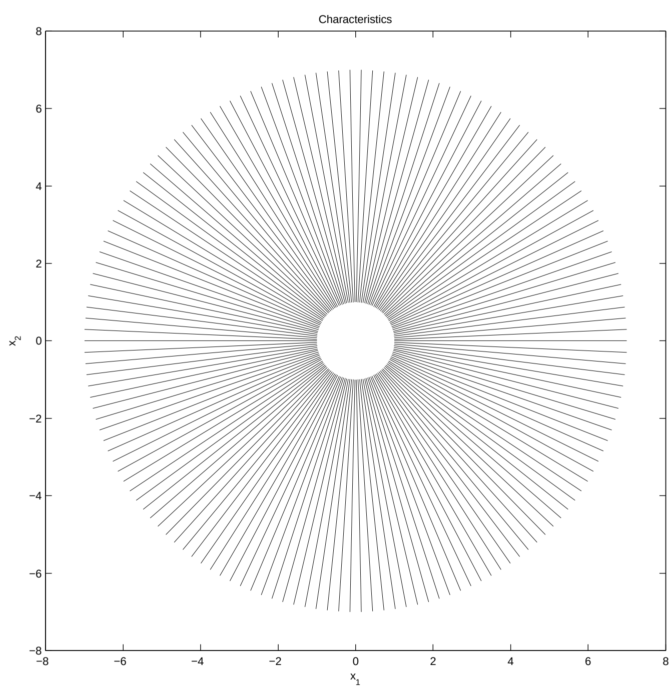


**Figure 5:** A set of characteristics for the wave equation for an expanding ring of waves.

**Comparisons** The numerical calculations of the Fourier transform solution and the Gaussian beam superpositions were carried out using a combination of Matlab and C. The Fourier transform solution will be used as the "true" solution to find the error in the wave field that is present in the Gaussian beam superpositions.

Figure 6 shows the absolute value of the difference between the Fourier transform solution and the Gaussian beam superpositions along $x_2 = 0$ at $t = 0$, while Figure 7 shows the same difference at $t = 2$. Note that the places where the error is highest correspond to the places where the amplitude has the largest gradient. This is in part the reason that the improvement in approximation of the initial data isn't as drastic as in the previous example. The numerically computed norms of the differences are given in Table 2.

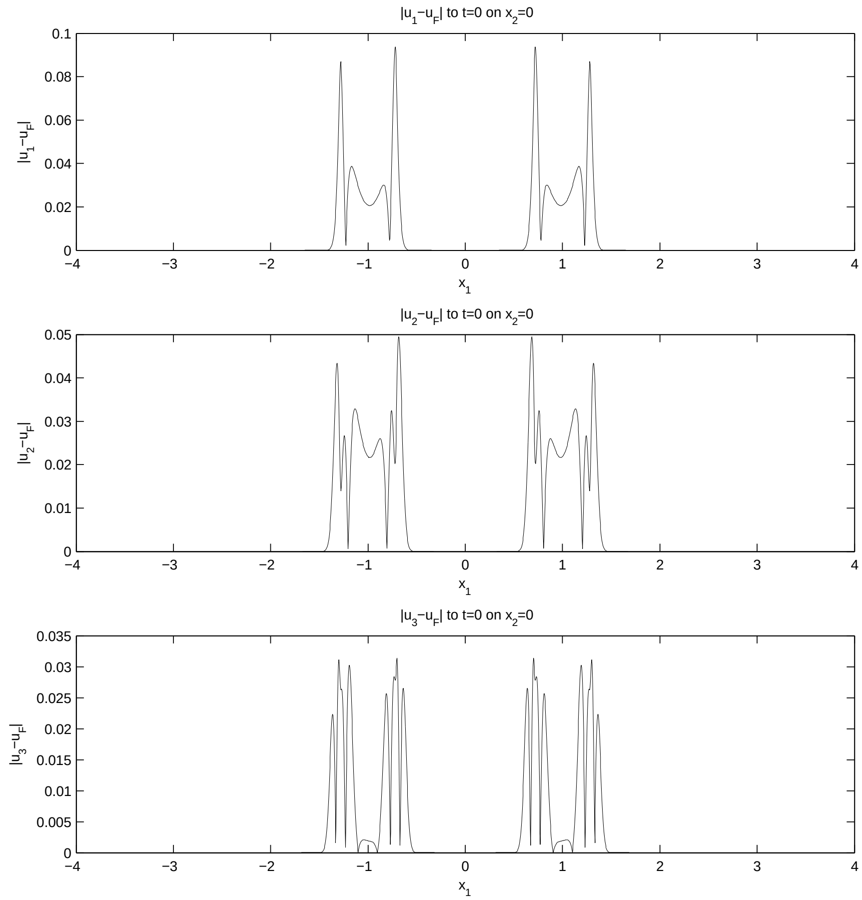


**Figure 6:** Differences between the Fourier transform solution and the Gaussian beam superposition solutions at $t = 0$ for $x_2 = 0$ for the expanding ring of waves example. Note that the scale for each graph is different.

| | Difference at $t = 0$ | | Difference at $t = 2$ | |
|---|---|---|---|---|
| | $L_2$-norm | $H_1$-norm | $L_2$-norm | $H_1$-norm |
| 1st order | 0.081412 | 17.8746 | 0.19086 | 41.8167 |
| 2nd order | 0.057496 | 12.6574 | 0.18761 | 41.5263 |
| 3rd order | 0.038806 | 8.5347 | 0.18640 | 41.3472 |

**Table 2:** Norm differences between the Fourier transform solution and the Gaussian beam superpositions for the expanding ring of waves example.

**Ray Divergence** As shown in Figure 5, for this particular initial data, the rays diverge quite a bit as time increases. However, since the accuracy of the Gaussian beam superposition depends on how well the initial data is resolved and how accurate the individual Gaussian beams are as solutions of the wave equation, the individual Gaussian beams interfere in just the right way to maintain an accurate solution. In other words,

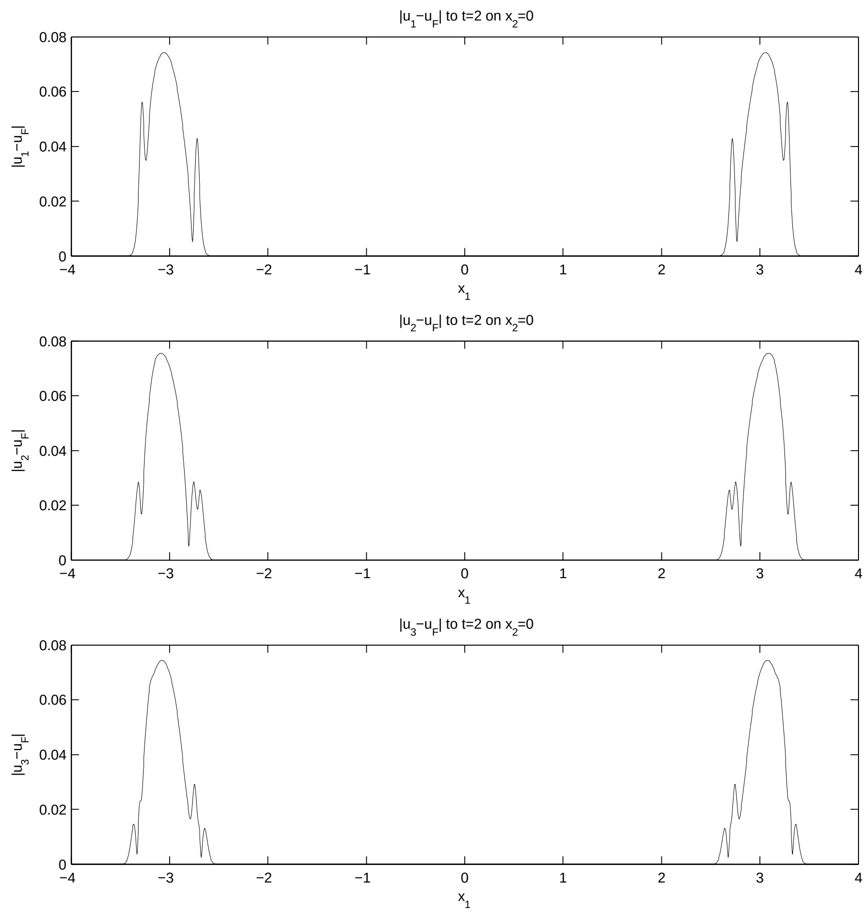


**Figure 7:** Differences between the Fourier transform solution and the Gaussian beam superposition solutions at $t = 2$ for $x_2 = 0$ for the expanding ring of waves example.

the Gaussian beams stretch in the direction in which the rays are diverging to fill in regions of low ray density (see Figure 8). We can see the result of this in Figure 9. While the beam centers are fairly far apart, they still provide an accurate solution.

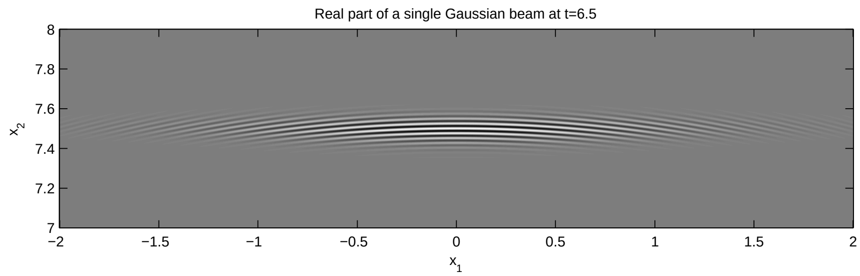


**Figure 8:** Real part of a single Gaussian beam used in the $u_3$ superposition at $t = 6.5$ for the expanding ring of waves example.

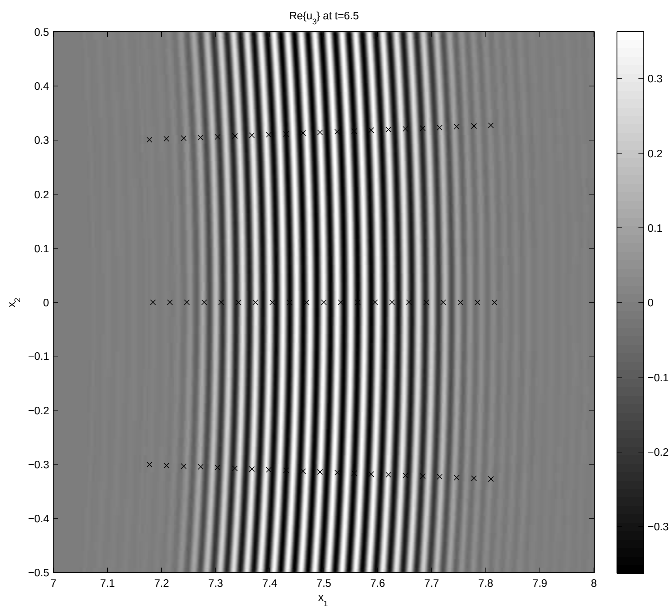


**Figure 9:** Real part of $u_3$ at $t = 6.5$ and the locations of the centers of the Gaussian beams used to construct the solution (marked by '$\times$') for the expanding ring of waves example. Notice that they are quite far apart.

## 3.4 Caustics

We consider an initial value problem for the constant coefficient wave equation (2) that exemplifies the strength of Gaussian beam superpositions. Let the initial data is given by

$$u_0(x) = e^{-100|x|^2 + ik(-x_1 + x_2^2)} \ ,$$

so that the initial phase and amplitude are,

$$\Phi(x) \quad = \quad -x_1 + x_2^2$$

and

$$A(x) \quad = \quad e^{-100|x|^2} \ .$$

The initial data for the time derivative of $u$, $u_{0t}$, is taken to give waves that propagate to the right. Since we are still working with the constant coefficient wave equation, the characteristics are straight lines. However, the phase is chosen in such a way so that the characteristics cross. Examining the initial data we see that the equations for the characteristics (8) give:

$$\begin{aligned} \mathcal{T} &= 2s\sqrt{1+4y_2^2} \\ \mathcal{X}_1 &= 2s + y_1 \\ \mathcal{X}_2 &= -4y_2 s + y_2 \ . \end{aligned}$$

The solution to the wave equation, will exhibit a caustic, when $(s, y_1, y_2)$ cannot be solved for in term of $(T, X_1, X_2)$. In other words, places where determinant of the Jacobian matrix of the transformation vanishes:

$$\begin{aligned} & \left| \begin{pmatrix} 2\sqrt{1+4y_2^2} & 0 & \frac{8sy_2}{\sqrt{1+4y_2^2}} \\ 2 & 1 & 0 \\ -4y_2 & 0 & 1-4s \end{pmatrix} \right| \\ = \ & 2\sqrt{1+4y_2^2}(1-4s) - \frac{8sy_2}{\sqrt{1+4y_2^2}}(-4y_2) \ . \end{aligned}$$

Setting this expression equal to 0, we get

$$\begin{aligned} 0 &= 2\sqrt{1+4y_2^2}(1-4s) + \frac{32sy_2^2}{\sqrt{1+4y_2^2}} \\ 0 &= (1+4y_2^2)(1-4s) + 16sy_2^2 \\ 0 &= 1 - 4s + 4y_2^2 \ . \end{aligned}$$

In the space time coordinates, $(T, X_1, X_2)$, this surface is given parametrically for $p \in [1/4, \infty)$, $q \in (-\infty, \infty)$ by

$$\begin{aligned} \mathcal{T} &= 4p^{3/2} \\ \mathcal{X}_1 &= 2p + q \\ \mathcal{X}_2 &= \pm(4p-1)^{3/2} \ . \end{aligned} \tag{11}$$

Since this is not a smooth surface, the solution to the wave equation develops a cusp caustic (see Figure 10).

The equations for the various Taylor coefficients that are needed to form Gaussian beams of first, second and third order are the same as in the previous section. Their superpositions are formed as before as well.

### 3.4.1 Numerical Calculations in the Presence of Caustics

Since the characteristics converge towards the $x_2$ axis, the $(x_1, x_2)$ support of the solution is compressed in the $x_2$ direction at the caustic and then it spreads apart once the rays have passed through the caustic (see Figure 11). The time series shown in Figure 11 is for a solution of the wave equation generated using a superposition of third order Gaussian beams. Note that since this solution is a superposition of Gaussian beams, it provides an accurate solution before, at and after the cusp caustic (at time $t = .5$). In fact, as can be seen from equations (11), after time $t = .5$ the solution is continuously passing through a caustic.

For the numerical calculations, a superposition of third order Gaussian beams is used to form the solution with $k = 10^4$. The superposition integral (10) is discretized using a 43 by 43 grid on $[-.2, .2] \times [-.2, .2]$ and the magnitude of the solution $|u|$ is evaluated on $[-.2, 1.2] \times [-.2, .2]$ using $1401 \times 401$ grid points.

### 3.4.2 Order of Magnitude of Wave Amplitude at Cusp Caustic

Maslov theory predicts that the order of magnitude of the solution to the wave equation at a cusp caustic is $O(k^{1/4})$ as $k \to \infty$. For a discussion of the asymptotic behavior of the solution, we refer the reader to [9], Chapter 6, and for a systematic classification of several types of caustics to Chapter 7, Section 9, of [4]. To verify this behavior numerically, we evaluate the Gaussian beam superposition at the tip of the caustic for several values of the large frequency parameter $k$. The superposition integral (10) is discretized on a parabolic grid centered about $(0, 0)$. That is, the grid points are located on the family of curves $y_1 = y_2^2 + c$. For

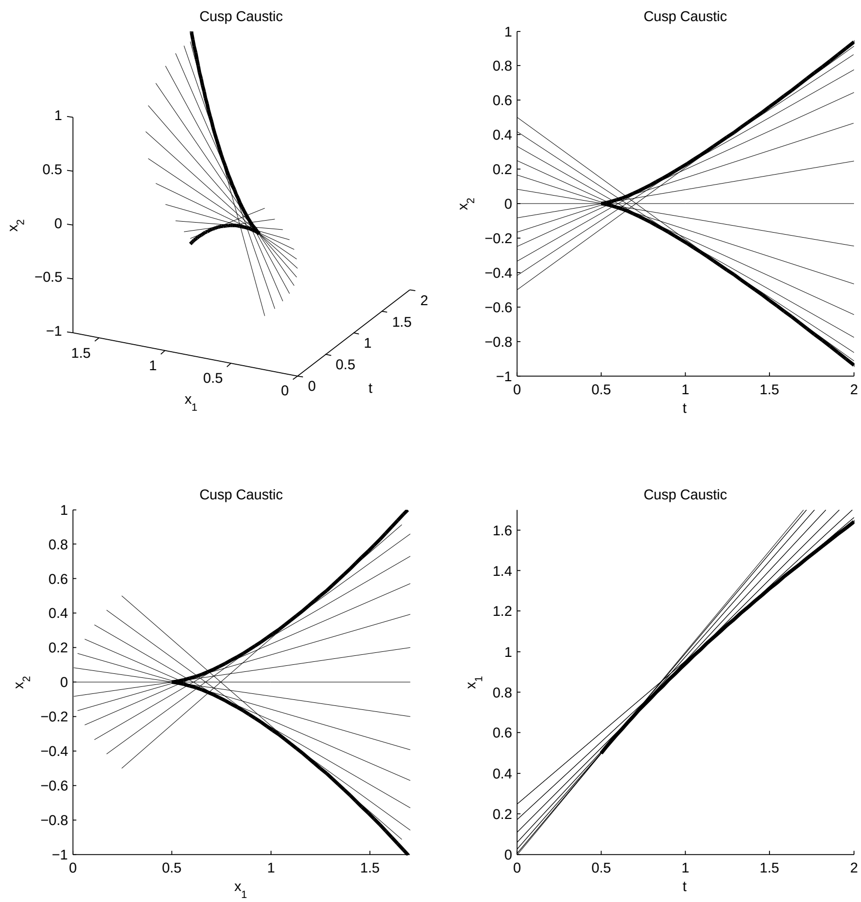


**Figure 10:** A set of rays that form a cusp caustic. The bold line shows the caustic set that is enveloped by this particular set of rays, which are shown by the gray lines.

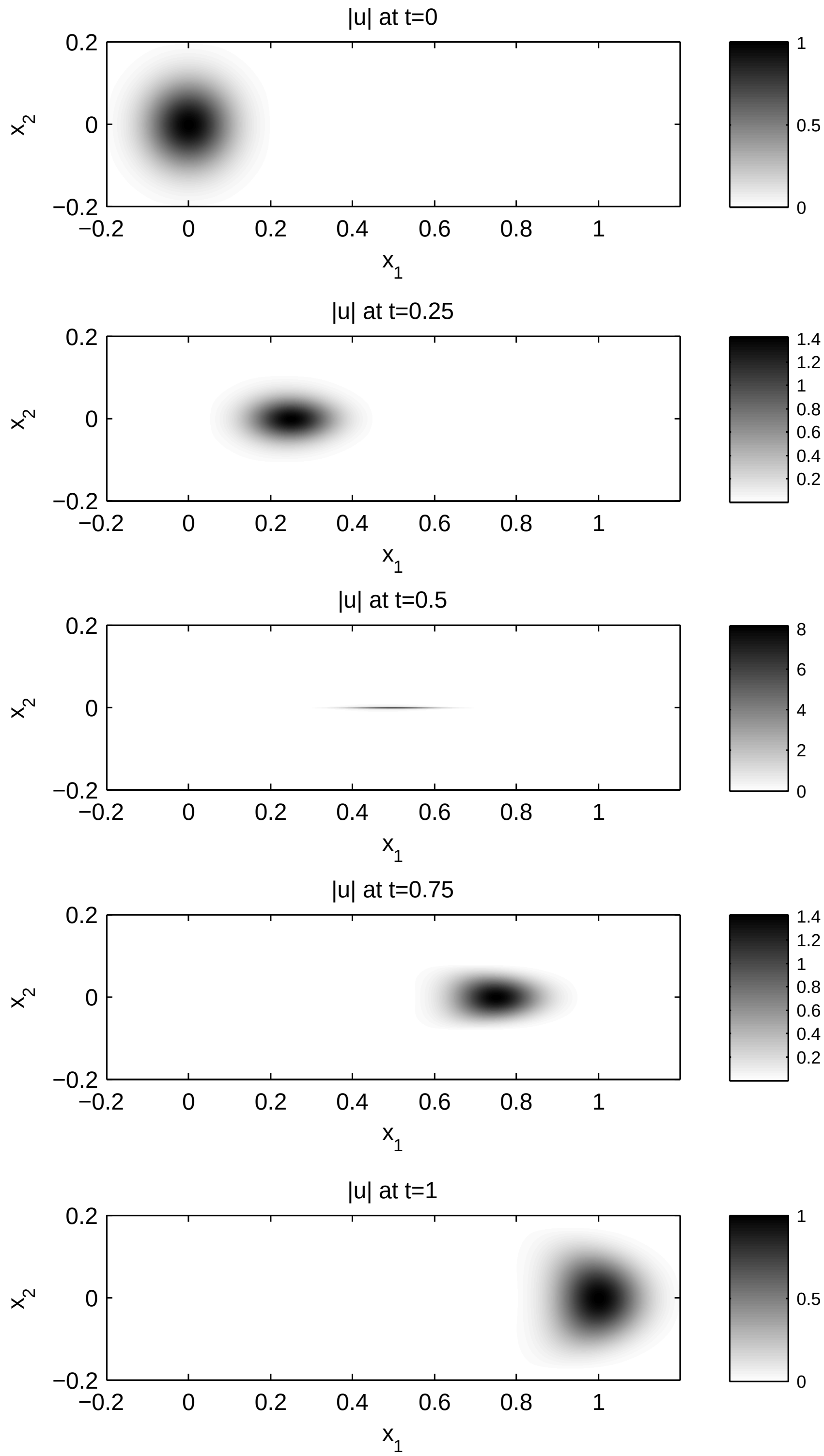


**Figure 11:** Time series of a solution of the wave equation with localized waves passing through a cusp caustic. Solution was computed using a superposition of third order Gaussian Beams.

the discretization in the $y_2$ direction, the interval $[-.2, .2]$ is discretized using an equispaced grid. The $y_1$ direction is discretized using the same distance between grip points as in the $y_2$ direction with 9 nodes. The exact numerical values used for the discretization are given in Table 3. The parabolic grid is used to minimize the calculation time and Gaussian beams that don't contribute to the solution magnitude are left out of the summation for the same reason.

| $k$ | $y_2$ Nodes | $\lvert u\rvert$ | $k$ | $y_2$ Nodes | $\lvert u\rvert$ |
|---|---|---|---|---|---|
| 1,000 | 13 | 3.2211 | 375,000 | 253 | 24.3562 |
| 1,250 | 15 | 3.5473 | 500,000 | 291 | 26.3072 |
| 2,500 | 21 | 4.7616 | 625,000 | 325 | 27.9141 |
| 3,750 | 27 | 5.6188 | 750,000 | 357 | 29.2916 |
| 5,000 | 31 | 6.2964 | 875,000 | 385 | 30.5038 |
| 6,250 | 33 | 6.8577 | 1,000,000 | 413 | 31.5905 |
| 7,500 | 37 | 7.3406 | 1,250,000 | 461 | 33.4858 |
| 8,750 | 39 | 7.7667 | 2,500,000 | 651 | 40.0677 |
| 10,000 | 43 | 8.1484 | 3,750,000 | 797 | 44.4634 |
| 12,500 | 47 | 8.8135 | 5,000,000 | 921 | 47.8569 |
| 25,000 | 65 | 11.1066 | 6,250,000 | 1,029 | 50.6588 |
| 37,500 | 81 | 12.6194 | 7,500,000 | 1,127 | 53.0648 |
| 50,000 | 93 | 13.7773 | 8,750,000 | 1,217 | 55.1849 |
| 62,500 | 103 | 14.7272 | 10,000,000 | 1,301 | 57.0876 |
| 75,000 | 113 | 15.5388 | 12,500,000 | 1,455 | 60.4102 |
| 87,500 | 123 | 16.2510 | 25,000,000 | 2,057 | 71.9804 |
| 100,000 | 131 | 16.8882 | 37,500,000 | 2,519 | 79.7282 |
| 125,000 | 147 | 17.9965 | 50,000,000 | 2,907 | 85.7177 |
| 250,000 | 207 | 21.8198 | | | |

**Table 3:** Details of the discretization used to obtain the magnitude of the wave equation solution at a cusp caustic.

A comparison between the theoretical asymptotic behavior of the magnitude of the solution and experimental results is shown is Figure 12. Note that the larger difference at the lower frequencies does not necessarily mean that the Gaussian beam superposition is providing an erroneous result. The Maslov prediction is an asymptotic one, so it may not be valid at the lower frequencies.

# 4 Transmission and Reflection of Gaussian Beams for the Wave Equation

In this section we consider the wave equation in $n$ space dimensions with a sound speed which is smooth up to either side of a codimension 1 hypersurface, $\Sigma$, but fails to be smooth across it. We assume that this surface is implicitly defined by some smooth function $\Psi$,

$$\Sigma = \{x : \Psi(x) = 0,\ \nabla\Psi(x) \neq 0\}\ ,$$

and that the sound speed $c(x)$ is given by

$$c(x) \quad = \quad \begin{cases} c^-(x) & \text{for} \quad \Psi(x) < 0 \\ c^+(x) & \text{for} \quad \Psi(x) > 0 \end{cases} \quad ,$$

for $c^+$, $c^- \in C^\infty(\mathbb{R}^n)$. We work in the high frequency regime and treat this problem as a transmission-reflection problem. Thus, we look for solutions of the wave equation

$$u_{tt} - c(x)\triangle u \quad = \quad 0 \text{ in } \mathbb{R}_t \times \mathbb{R}^n_x \tag{12}$$

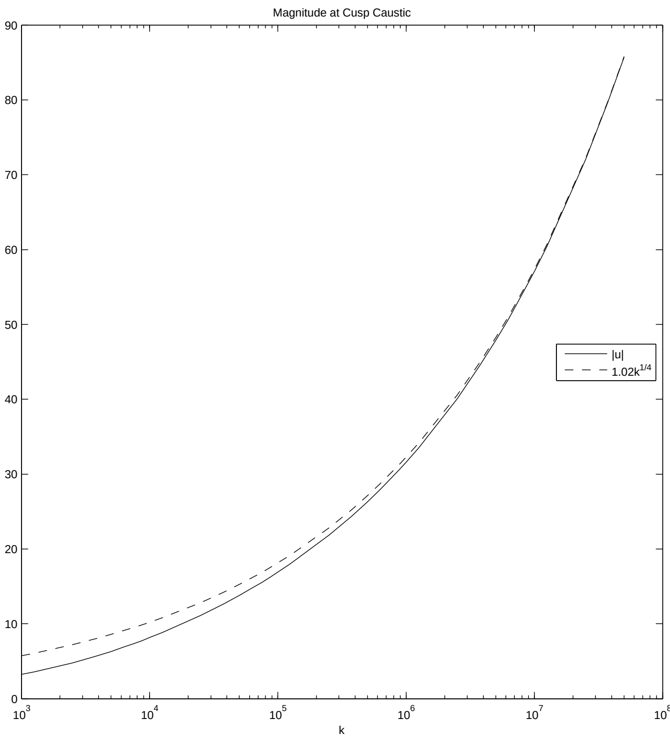


**Figure 12:** Comparison of the solution magnitude at a cusp caustic with Maslov theory prediction. Maslov theory predict that $|u| = O(k^{1/4})$. This behavior is present in the Gaussian beam superposition solution.

which consist of an incoming wave, a reflected wave, and a transmitted wave,

$$u \quad = \quad \begin{cases} u^I + u^R & \text{for} \quad \Psi(x) < 0 \\ u^T & \text{for} \quad \Psi(x) > 0 \end{cases} \quad , \tag{13}$$

locally near some point $x_0 \in \Sigma$.

## 4.1 Weak Formulation and the Matching Condition

For $u$ to be a distribution solution of (12), we need the following equations to hold on $\Sigma$

$$\begin{aligned} u^I + u^R &= u^T \\ \nabla u^I \cdot \nu + \nabla u^R \cdot \nu &= \nabla u^T \cdot \nu \ , \end{aligned} \tag{14}$$

for $\nu$ normal to $\Sigma$.

In what follows, we will use the notation

$$\begin{aligned} f_\nu &= \sum_{j=1}^{n} \nu_j f_{x_j} \ , \\ f_{\nu\nu} &= \sum_{j=1}^{n} \sum_{k=1}^{n} \nu_j f_{x_j x_k} \nu_k \ , \\ \nabla^\tau f &= \nabla f - f_\nu \nu \ . \end{aligned}$$

Now, we suppose that the three waves have the same form

$$\begin{aligned}
u^I &= A^I e^{ik\phi^I} = \left(a^{0I} + \frac{1}{k}a^{1I} + \ldots + \frac{1}{k^N}a^{NI}\right)e^{ik\phi^I} \ , \\
u^R &= A^R e^{ik\phi^R} = \left(a^{0R} + \frac{1}{k}a^{1R} + \ldots + \frac{1}{k^N}a^{NR}\right)e^{ik\phi^R} \ , \\
u^T &= A^T e^{ik\phi^T} = \left(a^{0T} + \frac{1}{k}a^{1T} + \ldots + \frac{1}{k^N}a^{NT}\right)e^{ik\phi^T} \ ,
\end{aligned}$$

with $k$ large and the phases and amplitudes independent of $k$. Note that this independence of $k$ and the matching condition equations (14) force

$$\phi^I = \phi^R = \phi^T$$

on $\Sigma$, see [2] Chapter 7, Section 7.2 for details and a physical interpretation. We assume that the incoming phase, $\phi^I$, and amplitudes, $a^{jI}$ are known and that $A^I$ is supported near $x_0$. Furthermore, we assume that $\phi^I_\nu(x_0) \neq 0$ and that $u^I$ is an asymptotically valid solution of (12) in $\Psi(x) < 0$.

## 4.2 Construction of the Incoming, Reflected and Transmitted Beams

We proceed as in the method of geometric optics. Substituting the form of the solution into the wave equation and equating powers of $k$, we get that each of the three phases $\phi^I$, $\phi^R$ and $\phi^T$ has to satisfy the eikonal equation,

$$|\phi_t|^2 - c(x)|\nabla\phi|^2 = 0 \ ,$$

in the appropriate domain. Since $\phi^I = \phi^R = \phi^T$ on $\Sigma$, all of the tangential derivatives of the three phases will agree on $\Sigma$. Thus, after substituting, we have that on $\Sigma$,

$$\begin{aligned}
|\phi^R_\nu|^2 &= |\phi^I_\nu|^2 \\
|\phi^T_\nu|^2 &= \frac{c^-|\phi^I_\nu|^2 - (c^+ - c^-)|\nabla^\tau\phi^I|^2}{c^+} \ .
\end{aligned} \tag{15}$$

Since $\nabla\phi$ gives the direction of propagation, to have a reflected wave and a transmitted wave, we need

$$\begin{aligned}
\phi^R_\nu &= -\phi^I_\nu \\
\phi^T_\nu &= \sqrt{\frac{c^-|\phi^I_\nu|^2 - (c^+ - c^-)|\nabla^\tau\phi^I|^2}{c^+}} \ .
\end{aligned}$$

These expressions give us the last piece of information necessary to solve the eikonal equations locally for $\phi^R$ and $\phi^T$ by the method of characteristics. Also they determine the Hessians of $\phi^R$ and $\phi^T$ except for $\phi^R_{\nu\nu}$ and $\phi^T_{\nu\nu}$ on $\Sigma$. We can obtain this last part by differentiating the eikonal equations in the $\nu$ direction. For each of the phases,

$$2\phi_t\phi_{t\nu} - 2c\nabla^\tau\phi\cdot\nabla^\tau\phi_\nu - 2c\phi_\nu\phi_{\nu\nu} - c_\nu|\nabla\phi|^2 = 0 \ ,$$

which gives,

$$\phi_{\nu\nu} = \frac{2\phi_t\phi_{t\nu} - c_\nu(x)|\nabla\phi|^2 - 2c\nabla^\tau\phi\cdot\nabla^\tau\phi_\nu}{2c\phi_\nu} \ . \tag{16}$$

Similarly, we can compute higher derivatives of the phases on $\Sigma$.

Now, we look at the amplitudes. To top order in $k$:

$$\begin{aligned}
a^{0I} + a^{0R} &= a^{0T} \\
a^{0I}\phi^I_\nu + a^{0R}\phi^R_\nu &= a^{0T}\phi^T_\nu \ .
\end{aligned} \tag{17}$$

Since we have already determined the $\nu$ derivatives of the phases on $\Sigma$, these equations can be used to obtain $a^{0R}$ and $a^{0T}$ on $\Sigma$, which serve and an initial condition for the transport equations for the highest order reflected and transmitted amplitudes:

$$2\phi_t a^0_t + \phi_{tt}a^0 - c(x)a^0\triangle\phi - 2c(x)\nabla\phi\cdot\nabla a^0 = 0 \ . \tag{18}$$

As in the case for the phases, we have local existence for the amplitudes, and as before we can determine the derivatives of the amplitudes on $\Sigma$ by differentiating equations (17) and the transport equation (18).

The next order amplitudes satisfy

$$\begin{aligned} a^{1I} + a^{1R} &= a^{1T} \\ a^{1I}\phi^I_\nu + a^{0I}_\nu + a^{1R}\phi^R_\nu + a^{0R}_\nu &= a^{1T}\phi^T_\nu + a^{0T}_\nu \ , \end{aligned} \tag{19}$$

which again give the necessary initial conditions for the next order transport equations. In this fashion, we can continue until we have determined the amplitudes up to order $N$; thus constructing a local asymptotic solution of (12) of the form (13). We remark that these equations provide the necessary initial conditions for the construction global Gaussian beam solutions of the form (13). There is only one technical point that needs to be addressed. Since Gaussian beams determine the amplitude and phase functions up to high order in $k$, the matching conditions (14) will only be satisfied to a high order in $1/k$. This is not enough however, since for the form (13) to be a weak solution of the wave equation (2) the matching condition has to hold exactly. To correct this, we take the difference between the wave field for $\Psi < 0$ and $\Psi > 0$ on $\Sigma$ and extend it smoothly to a function on all of $\mathbb{R}^n$. This function can then be added to the Gaussian beam solution to make it a true weak solution of the wave equation. This function will not affect the asymptotics as it is of high order in $1/k$.

### 4.3 Snell's Law, Total Internal Reflection, Reflection and Transmission Coefficients

Suppose that

$$c(x) = \begin{cases} c^- & \text{for} \quad x_n < 0 \\ c^+ & \text{for} \quad x_n > 0 \end{cases} .$$

Thus, $\nu$ points in the $x_n$ direction and $\Sigma$ is the hyperplane $x_n = 0$. Let $\nabla'$ be the gradient in $x_1, \dots, x_{n-1}$ and compute

$$\begin{aligned} \phi^R_{x_n} &= -\phi^I_{x_n} \\ \phi^T_{x_n} &= \sqrt{\frac{(c^- - c^+)|\nabla'\phi^I|^2 + c^-|\phi^I_{x_n}|^2}{c^+}} \ , \end{aligned}$$

for $x_n = 0$. Note that the incoming, reflected and transmitted waves lie in the same plane (see Figure 13).

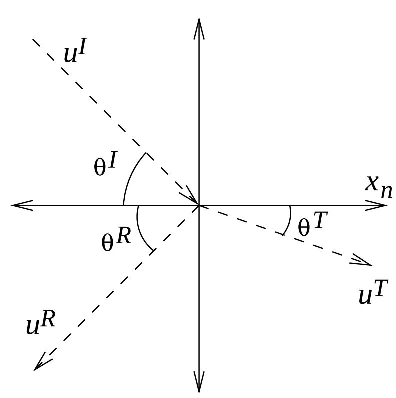


**Figure 13:** Incoming, reflected and transmitted Gaussian beams.

We calculate:

$$\begin{aligned}
\sin(\theta^I) &= \frac{|\nabla'\phi^I|}{|\nabla\phi^I|} \\
\sin(\theta^R) &= \frac{|\nabla'\phi^R|}{|\nabla\phi^R|} = \frac{|\nabla'\phi^I|}{|\nabla\phi^I|} = \sin(\theta^I) \\
\sin(\theta^T) &= \frac{|\nabla'\phi^T|}{|\nabla\phi^T|} = \sqrt{\frac{c^+}{c^-}}\frac{|\nabla'\phi^I|}{|\nabla\phi^I|} = \sqrt{\frac{c^+}{c^-}}\sin(\theta^I) \ .
\end{aligned}$$

Thus, we have obtained the familiar "angle of incidence equals angle of reflection" and Snell's law:

$$\begin{aligned}
\theta^R &= \theta^I \\
\frac{\sin(\theta^T)}{\sqrt{c^+}} &= \frac{\sin(\theta^I)}{\sqrt{c^+}} \ .
\end{aligned}$$

Total internal reflection occurs when $\phi^T_{x_n}$ is complex, as in that case the transmitted wave just decays exponentially in $x_n$:

$$\begin{aligned}
\frac{(c^- - c^+)|\nabla'\phi^I|^2 + c^-|\phi^I_{x_n}|^2}{c^+} &\leq 0 \\
c^-|\nabla\phi^I|^2 &\leq c^+|\nabla'\phi^I|^2 \\
\sqrt{\frac{c^-}{c^+}} &\leq \sin(\theta^I) \ .
\end{aligned}$$

Thus the critical angle for total internal reflection is

$$\arcsin\left(\sqrt{\frac{c^-}{c^+}}\right) \ .$$

Note that for total internal reflection to occur $c^- < c^+$.

The reflection and transmission coefficients measure what fraction of the incident amplitude is transmitted and what fraction is reflected. From (17), we readily compute:

$$\begin{aligned}
a^{0R} &= \frac{1 - \phi^I_{x_n}/\phi^T_{x_n}}{1 + \phi^I_{x_n}/\phi^T_{x_n}}\ a^{0I} \equiv Ra^{0I} \\
a^{0T} &= \frac{2}{1 + \phi^T_{x_n}/\phi^I_{x_n}}\ a^{0I} \equiv Ta^{0I} \ .
\end{aligned}$$

At normal incidence (*i.e.* $|\nabla\phi^I|^2 = |\phi^I_{x_n}|^2$ ), the transmission and reflection coefficients become

$$\begin{aligned}
R &= \frac{1 - c^+/c^-}{1 + c^+/c^-} = \frac{c^- - c^+}{c^- + c^+} \\
T &= \frac{2}{1 + c^-/c^+} = \frac{2c^+}{c^- + c^+} \ .
\end{aligned}$$

## 4.4 Lipschitz Continuous Sound Speed

We now restrict our attention to two space dimensions and a particular sound speed given by

$$c(x) = |x_2| + 1 \ .$$

In this case, $\nu$ is in the $x_2$ direction and $\Sigma$ is given by $x_2 = 0$. On $\Sigma$, the $x_2$ derivatives of the phases, given by equation (15), are

$$\begin{aligned}
\phi^R_{x_2} &= -\phi^I_{x_2} \\
\phi^T_{x_2} &= \phi^I_{x_2}
\end{aligned}$$

and the second derivative $\phi^T_{x_2x_2}$, given by equation (16), is

$$\phi^T_{x_2x_2} = \phi^I_{x_2x_2} - \frac{|\nabla\phi^I|^2}{\phi^I_{x_2}} .$$

Looking at the amplitude relations (17), we obtain

$$\begin{aligned} a^{0R} &= 0 \\ a^{0T} &= a^{0I} \end{aligned}$$

and equation (18) gives,

$$a^{0I}(\phi^T_{x_2x_2} - \phi^I_{x_2x_2}) + 2\phi^I_{x_2}(a^{0T}_{x_2} - a^{0I}_{x_2}) = 0 .$$

For the next order amplitudes, equations (19) give us

$$\begin{aligned} a^{1R} &= -\frac{1}{4(\phi^I_{x_2})^3}|\nabla\phi^I|^2 a^{0I} \\ a^{1T} &= a^{1I} - \frac{1}{4(\phi^I_{x_2})^3}|\nabla\phi^I|^2 a^{0I} . \end{aligned}$$

Therefore, in this case, we see that to top order the incoming wave is transmitted and the reflected wave's amplitude is one order lower in $k$ than the incident wave. One can carry out the same argument to find that if the sound speed is smooth up to order $l$ across the interface $\Sigma$ then the reflected wave would have an amplitude which is $l+1$ orders lower in $k$.

# 5 Conclusion

We have shown that integral superpositions of Gaussian beams can be used to approximate the initial data for PDE. Thus, through the well-posedness of the PDE, the integral superposition gives an approximate solution. In particular, we have proved a well-posedness estimate for the wave equation and used a Gaussian beam superposition to approximate the solution to the 2-D wave equation for an expanding ring of waves. The Gaussian beams in this particular case stretch to fill in the gaps that result due to the divergence in the rays. In traditional geometric optics methods, one would need to insert more rays to resolve the wave field in such places. Since this is not necessary in the presented method, this example shows the power of the Gaussian beam method.

Another advantage of the Gaussian beam method is that the obtained solution is global. This means that even in the presence of caustics the Gaussian beam solution is valid, before, after and at the caustic region. As an example, we have computed the order of magnitude of the solution at a cusp caustic as a function of the high frequency parameter and compared it to the asymptotic behavior predicted by Maslov theory. While in geometric optics methods the solution can be extended past caustics by using a phase correction, a computation of the solution at a caustic is not possible. The identification of caustics and their corrections are non-trivial in standard geometric optics. Using Gaussian beams, one can easily compute the global wave field.

Lastly, we have shown how one can find a Gaussian beam solution in the case of non-smooth sound speed as a superposition of an incoming, transmitted and reflected beam. This construction is in parallel with the construction for standard geometric optics. We have used this solution to derive Snell's law, find the angle of total internal reflection and compute reflection and transmission coefficients. We have also shown that the order of discontinuity of the sound speed determines the order of magnitude of the reflected beam.

# Acknowledgments

The author acknowledges the financial support of the National Science Foundation (UCLA VIGRE Grant No. DMS-0502315 and UTA RTG Grant No. DMS-0636586) and the UCLA Mathematics Department.

# References


[1] V. Červený, M. Popov, and I. Pšenčík. Computation of wave fields in inhomogeneous media - gaussian beam approach. *Geophys. J. R. Astr. Soc.*, Vol. 70:109–128, 1982.

[2] F. S. Crawford, Jr. *Waves*, volume Vol. 3 of *The Berkeley Physics Course*. McGraw-Hill, 1968.

[3] L. C. Evans. *Partial Differential Equations*, volume Vol. 19 of *Graduate Studies in Mathematics*. American Mathematical Society, 1998.

[4] V. Guillemin and S. Sternberg. *Geometric Asymptotics*, volume Vol. 14 of *Mathematical Survey and Monographs*. American Mathematical Society, 1977.

[5] N. R. Hill. Prestack gaussian-beam depth migration. *Geophysics*, Vol. 66(4):1240–1250, 2001.

[6] L. Hörmander. On the existence and the regularity of solutions of linear pseudo-differential equations. *L'Enseignement Mathématique*, XVII:99–163, 1971.

[7] J. Ralston. Gaussian beams and the propagation of singularities. *Sudies in PDE, Stud. Math.*, 23:206–248, 1982.

[8] N. M. Tanushev, J. Qian, and J. V. Ralston. Mountain waves and gaussian beams. *SIAM Multiscale Modeling and Simulation*, Vol. 6(2):688–709, 2007.

[9] M. E. Taylor. *Partial Differential Equations I: Basic Theory*, volume 115 of *Applied Mathematical Sciences*. Springer-Verlag, 1996.